

X80K-01

62 63986

Copy 40
RM SL56G23

Declassified by authority of NASA
Classification Change Notices No. 167
Dated ** 1/16/69



RESEARCH MEMORANDUM

for the
U. S. Air Force

DECLASSIFIED- AUTHORITY MEMO U.S.
4908
RICE TO SHAUKLAS DATED 11/21/68

DRAG AT MODEL TRIM LIFT OF A 1/15-SCALE
CONVAIR B-58 SUPERSONIC BOMBER
By Russell N. Hopko and William H. Kinard
Langley Aeronautical Laboratory
Langley Field, Va.

X30-71300

(THRU) 31 (CATEGORY)

(CODE)

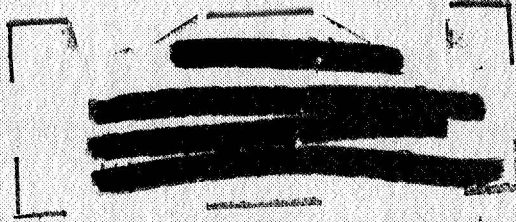
(ACCESSION NUMBER) 31 (PAGES)

(NASA CR OR TMX OR AD NUMBER)

Restriction/Classification Cancelled

F No. 602(A)

ICE REPORT



NATIONAL ADVISORY COMMITTEE FOR AERONAUTICS

WASHINGTON

JUL 13 1956

NATIONAL ADVISORY COMMITTEE FOR AERONAUTICS

RESEARCH MEMORANDUM

for the

U. S. Air Force

DRAG AT MODEL TRIM LIFT OF A 1/15-SCALE

CONVAIR B-58 SUPERSONIC BOMBER

By Russell N. Hopko and William H. Kinard


SUMMARY

An investigation has been made by the Langley Pilotless Aircraft Research Division utilizing a 1/15-scale rocket-propelled model of the Convair B-58 supersonic bomber. The drag at model trim lift was obtained at Mach numbers between 0.85 and 2.0 at corresponding Reynolds number per foot of 3.5×10^6 and 13.7×10^6 , respectively. The results of the present investigation are compared with unpublished data obtained from several facilities, WADC 10-foot tunnel, Ames 6- by 6-foot supersonic tunnel and the Langley 16-foot transonic tunnel. A comparison of the drag at transonic speeds and at approximately the same Reynolds numbers showed excellent agreement. A drag coefficient of 0.028 at a Mach number of 2.0 was obtained at zero-lift conditions.

INTRODUCTION

At the request of the U. S. Air Force, the Langley Pilotless Aircraft Research Division has undertaken a flight test program to determine the drag near zero lift of the Convair B-58 composite airplane. The vehicle portion of the B-58 supersonic bomber consists of two parts; the basic inhabited airframe which is designated the return component, and an expendable pod which is an air-to-surface missile. The complete vehicle with pod attached on a short pylon is designated the composite airplane.

The return component consists of a 60° modified delta wing at 3° of incidence incorporating 0.15-local-semispan leading-edge camber, a Mach number 2.0 supersonic "area rule" fuselage, and a swept tapered vertical tail mounted atop the fuselage aft of the wing trailing edge. Four nacelles are pylon mounted underneath the wing.



The expendable pod is essentially a body-of-revolution missile with the supporting pylon attached to its upper surface. Aerodynamic surfaces of the pod, canard and wing, are 60° deltas with 10° swept trailing edges and the vertical tails are swept and tapered.

Results of some previous investigations during the development of the B-58 have been reported in references 1 to 3. In the present investigation a 1/15-scale rocket-propelled composite model was flown and data were obtained over a Mach number range of 0.85 to 2.0 at corresponding Reynolds number per foot of 3.5×10^6 and 13.7×10^6 , respectively. This investigation was conducted at the Langley Pilotless Aircraft Research Station at Wallops Island, Va.

SYMBOLS

A	cross-sectional area
A_L	longitudinal acceleration, ft/sec ²
g	acceleration due to gravity, ft/sec ²
C_c	chord-force coefficient, $\frac{\text{Chord force}}{qS}$
C_D	drag coefficient, $\frac{\text{Drag}}{qS}$
C_{DI}	internal drag coefficient, $\frac{\text{Internal drag}}{qS}$
C_{DE}	external drag coefficient, $C_{DT} - C_{DI} - C_{DB}$
C_{DB}	base drag coefficient, $\frac{P_o - P_b}{q} \times \frac{S_b}{S}$
C_{DT}	total drag coefficient, $C_{DB} + C_{DI} + C_{DE}$
b	span
C_N	normal-force coefficient, $\frac{\text{Normal force}}{qS}$
M	Mach number
l	overall length

P_o	static pressure, lb/sq ft
P_b	base pressure, lb/sq ft
q	dynamic pressure, lb/sq ft
R	Reynolds number
S	total wing area including body intercept, 6.86 sq ft
S_b	area of nacelle base (four nacelles)
t	time
V	velocity, ft/sec
W	model weight, lb
γ	angle between instantaneous flight path and the horizontal, deg

MODEL

The general arrangement of the model is shown in figure 1 and a photograph of the model is shown in figure 2. Other pertinent physical characteristics are presented in tables I, II, and III. The wing, constructed mainly of steel, has a diamond plan form with 60° sweep of the leading edge and a -10° sweep of the trailing edge. Outboard of station 3.33 the wing has an NACA 0004.08-63 airfoil section; at the root it has an NACA 0003.46-64.069 section. The wing has 3° of incidence and dihedral of $2^\circ 13' 45''$ outboard of station 3.767. The camber has been designed for a lift coefficient of 0.22 at a Mach number of 1.414. The elevon deflection was 0° .

The pod wing and canard are of similar plan form to the wing of the return component and have NACA 0004.5-64 airfoil sections. These surfaces were at 0° deflection for the present investigation.

The vertical tail is a swept tapered surface with an NACA 0005-64 airfoil section. The leading-edge sweep is 52° and the taper ratio is 0.324.

The pod tail is a swept tapered surface with an NACA 0005-64 section. The leading edge is swept 60° and the taper ratio is 0.35.

The model was constructed by ^{Convair, Division of General Dynamics Corp.} ~~the Consolidated Vultee Aircraft Corp.~~, Ft. Worth, Texas.

TEST PROCEDURE

Instrumentation

The models were internally instrumented by the Langley Aeronautical Laboratory of the National Advisory Committee for Aeronautics with an eight-channel telemeter which transmitted the following information: longitudinal acceleration (two instruments), normal acceleration, transverse acceleration, total pressure (two instruments), static pressure, and base pressure. The base pressure measurements were made on one inboard nacelle by using four pressure orifices manifolded together and connected to a pressure pickup instrument. A modified SCR-584 radar unit was used to determine the space position of the model in flight. The velocity was obtained with a CW Doppler velocimeter and a rawinsonde provided atmospheric conditions and winds aloft velocities throughout the altitude range transversed by the model in flight.

Propulsion

The model attained a maximum Mach number of approximately 2.0 with an M-5 Jato (Nike booster). After burnout the booster drag separated from the model and data were obtained during coasting flight. A photograph of the model in launching position is shown in figure 3.

DATA REDUCTION

Ground Radar

Drag coefficients were obtained during model flight by evaluating the following expression

$$C_D = \frac{W}{gqS} \left(\frac{dV}{dt} + g \sin \gamma \right)$$

where V is the velocity obtained from CW Doppler velocimeter and corrected to the tangential velocity along the flight path and also corrected for winds of the altitudes traversed in flight.

Telemeter

The longitudinal accelerometer data were used in the following equation

$$C_c = \frac{A_l}{g} \frac{W/S}{q}$$

A similar expression was used to evaluate the normal and side-force coefficients using the normal and transverse accelerations, respectively.

The base drag coefficients were determined from

$$C_{DB} = \frac{P_o - P_b}{q} \frac{S_b}{S}$$

ACCURACY

The accuracies in coefficient form for the Mach number, drag, and normal-force data are estimated to be

M	C_{DT}	C_N	M
2	± 0.0005	± 0.008	± 0.01
1	± 0.0008	± 0.013	± 0.01

RESULTS AND DISCUSSION

The Reynolds numbers per foot are given in figure 4. The total drag coefficients for the configuration are shown in figure 5. These drag coefficients were determined by both CW Doppler radar and telemetered accelerations. The data range of the Doppler radar was from $M = 2$ to $M = 1.5$ for this investigation; the data range of the telemeter was from $M = 2$ to $M = 0.85$. Excellent agreement was obtained between the Doppler and telemeter data. Base pressures were measured on one inboard nacelle and these data reduced to drag coefficient are shown in figure 6. Also shown in figure 6 are base pressure measurements on both the inboard and outboard nacelles, obtained in the Langley 16-foot transonic tunnel and the Ames 6- by 6-foot supersonic tunnel. Inasmuch as the outboard nacelle base pressures were not measured in flight and because the comparison of the flight and tunnel base pressure measurements for the inboard nacelle shows excellent agreement, the outboard nacelle base pressure measurements obtained in the Langley 16-foot transonic tunnel were employed in evaluating the external drag data for the present rocket model.

No measurements of the internal drag were made with the flight model. The internal drag measurements obtained in the Langley 16-foot transonic tunnel on both the inboard and outboard nacelles are shown in figure 7. Also shown are internal drag measurements obtained in the Langley 4- by 4-foot supersonic pressure tunnel on one outboard nacelle of a similar


nacelle configuration. The inlet spike for the 16-foot-transonic-tunnel investigation was set at the $M = 0.9$ cruise position giving a mass-flow ratio of approximately 0.9. For the present investigation the inlet spikes were set for approximately the flight condition at $M = 2$ with a respective mass-flow ratio of 1.0 and the mass-flow ratios of subsonic speeds were approximately 0.7. Therefore, calculated values of the internal drag using one-dimensional-flow theory and also reference 4 were used to determine the external drag in this investigation.

A comparison of available external drag data is made in figure 8 ^{which shows} ~~the~~ ^{the} drag coefficient at model trim lift (shown in fig. 9) and essentially zero sideslip, as determined from the transverse accelerations, ^{and} is presented and compared with data obtained at WADC 10-foot tunnel, Langley 16-foot transonic tunnel, and Ames 6- by 6-foot supersonic tunnel; the data of the latter configuration were obtained with the inboard nacelles parallel to the wing chord and the outboard nacelles at -5° to the wing chord. The configuration tested in the Langley 16-foot transonic tunnel was similar to the configuration of this investigation. A comparison of the external drag obtained in this investigation with the results obtained in the 16-foot transonic tunnel at approximately the same Reynolds numbers showed excellent agreement. The 6- by 6-foot tests were made with fixed transition and a ΔC_D of approximately 0.0014 due to the boundary-layer trip was estimated. This increment in drag coefficient has not been subtracted from the data obtained in the Ames 6- by 6-foot supersonic tunnel presented herein.

A nondimensional cross-sectional area diagram of the present configuration is shown in figure 10.

CONCLUDING REMARKS

The drag at model trim lift of the Convair B-58 supersonic bomber was obtained at Mach numbers between 0.85 and 2.0 at corresponding Reynolds number per foot of 3.5×10^6 and 13.7×10^6 . The external drag of the model at trim lift has been compared with data obtained in the Langley 16-foot transonic tunnel. A comparison of the drag at transonic speeds and at approximately the same Reynolds number showed excellent agreement. A drag coefficient of 0.028 at a Mach number of 2.0 was



obtained at zero-lift conditions. The model had a mild transonic trim change. ~~with a drag rise Mach number of approximately 0.95.~~

Langley Aeronautical Laboratory,
National Advisory Committee for Aeronautics,
Langley Field, Va., June 27, 1956.

Russell N. Hopko
Russell N. Hopko

Aeronautical Research Scientist

William H. Kinard
William H. Kinard

Aeronautical Research Scientist

Approved:

for *J. A. Shortal*
Joseph A. Shortal
Chief of Pilotless Aircraft Research Division

mhg

REFERENCES

1. Hall, James R., and Hopko, Russell N.: Drag and Static Stability at Low Lift of Rocket-Powered Models of the Convair MX-1626 Airplane at Mach Numbers From 0.7 to 1.5. NACA RM SL53F09a, U. S. Air Force, 1953.
2. Swihart, John M., and Foss, Willard E., Jr.: Transonic Aerodynamic and Trim Characteristics of a Multi-Engine Delta-Wing Airplane Model. NACA RM L55I27b, 1956.
3. Hopko, Russell N.: Drag Near Zero Lift of a 1/7-Scale Model of the Convair B-58 External Store as Measured in Free Flight Between Mach Numbers of 0.8 and 2.45. NACA RM SL55G22a, U. S. Air Force, 1955.
4. Fraenkel, L. E.: Some Curves for Use in Calculations of the Performance of Conical Centrebody Intakes at Supersonic Speeds and at Full Mass Flow. Tech. Note No. Aero. 2135, British R.A.E., Dec. 1951.

TABLE I

WING GEOMETRY

[Trailing-edge radius, 0.010 typical; see figure 1(b)]

Span station 3.767 Chord = 36.216		Span station 10.667 Chord = 23.048		Span station 15.835 Chord = 13.189		Span station 18.150 Chord = 8.768		Span station 20.667 Chord = 3.965		Root chord Chord = 42.741			
"B" dimension	Upper ordinate	Lower ordinate	"B" dimension	Upper ordinate	Lower ordinate	"B" dimension	Upper ordinate	Lower ordinate	"B" dimension	Upper ordinate	Lower ordinate	Distance	Ordinate
0	-0.063	-0.108	0	-0.304	-0.304	0	-0.424	-0.424	0	-0.589	-0.589	0	0
.416	.194	-.261	.288	-.080	-.389	.165	-.301	-.479	.051	-.547	-.600	.534	.284
.889	.320	-.327	.576	.061	-.400	.277	-.253	-.478	.099	-.517	-.592	1.069	.501
1.811	.445	-.445	1.128	.179	-.381	.559	-.159	-.466	.197	-.475	-.570	2.137	.401
2.716	.526	-.526	1.728	.295	-.392	1.533	.007	-.425	.299	-.437	-.549	3.206	.468
3.621	.586	-.586	2.304	.355	-.392	2.064	.111	-.382	.397	-.405	-.533	4.274	.519
5.432	.667	-.667	3.461	.421	-.421	2.712	.176	-.345	.595	-.427	-.501	6.411	.596
7.243	.711	-.711	4.611	.451	-.451	4.098	.256	-.288	.792	-.320	-.469	8.488	.648
10.865	.739	-.739	6.915	.467	-.467	5.275	.262	-.262	1.189	-.320	-.416	12.822	.715
14.486	.719	-.719	9.219	.456	-.456	6.594	.242	-.242	1.587	-.208	-.363	17.388	.739
18.108	.666	-.666	11.525	.421	-.421	7.913	.211	-.211	1.984	-.171	-.309	21.009	.719
21.729	.580	-.580	13.830	.368	-.368	9.232	.171	-.171	2.379	-.159	-.281	24.631	.666
25.351	.469	-.469	16.134	.296	-.296	10.551	.122	-.122	2.776	-.117	-.219	28.253	.580
28.973	.335	-.335	18.438	.211	-.211	11.187	.066	-.066	3.173	-.096	-.173	31.874	.469
32.594	.182	-.182	20.744	.115	-.115	12.529	.036	-.036	3.568	-.085	-.128	35.460	.335
34.405	.098	-.098	21.896	.064	-.064	13.189	0	0	3.768	-.080	-.107	39.117	.182
36.216	0	0	23.048	0	0	L.E. radius	.024	0	3.965	-.075	-.091	40.928	.098
			L.E. radius	.042	0	L.E. radius			L.E. radius	.007		42.741	0

TABLE III

PHYSICAL CHARACTERISTICS OF THE MODEL

Wing:

Area (included), sq in.	987.26
Span, in.	45.49
Aspect ratio	2.096
Mean aerodynamic chord, in.	28.94
Sweepback of leading edge, deg	60
Trailing edge sweep, deg	-10
Incidence, deg	+3
Airfoil section	NACA 0004.08-63

Vertical tail:

Area, sq in.	102.4
Aspect ratio	2.64
Sweepback of leading edge, deg	52
Airfoil section	NACA 0005-64
Taper ratio	0.324

Pod wing:

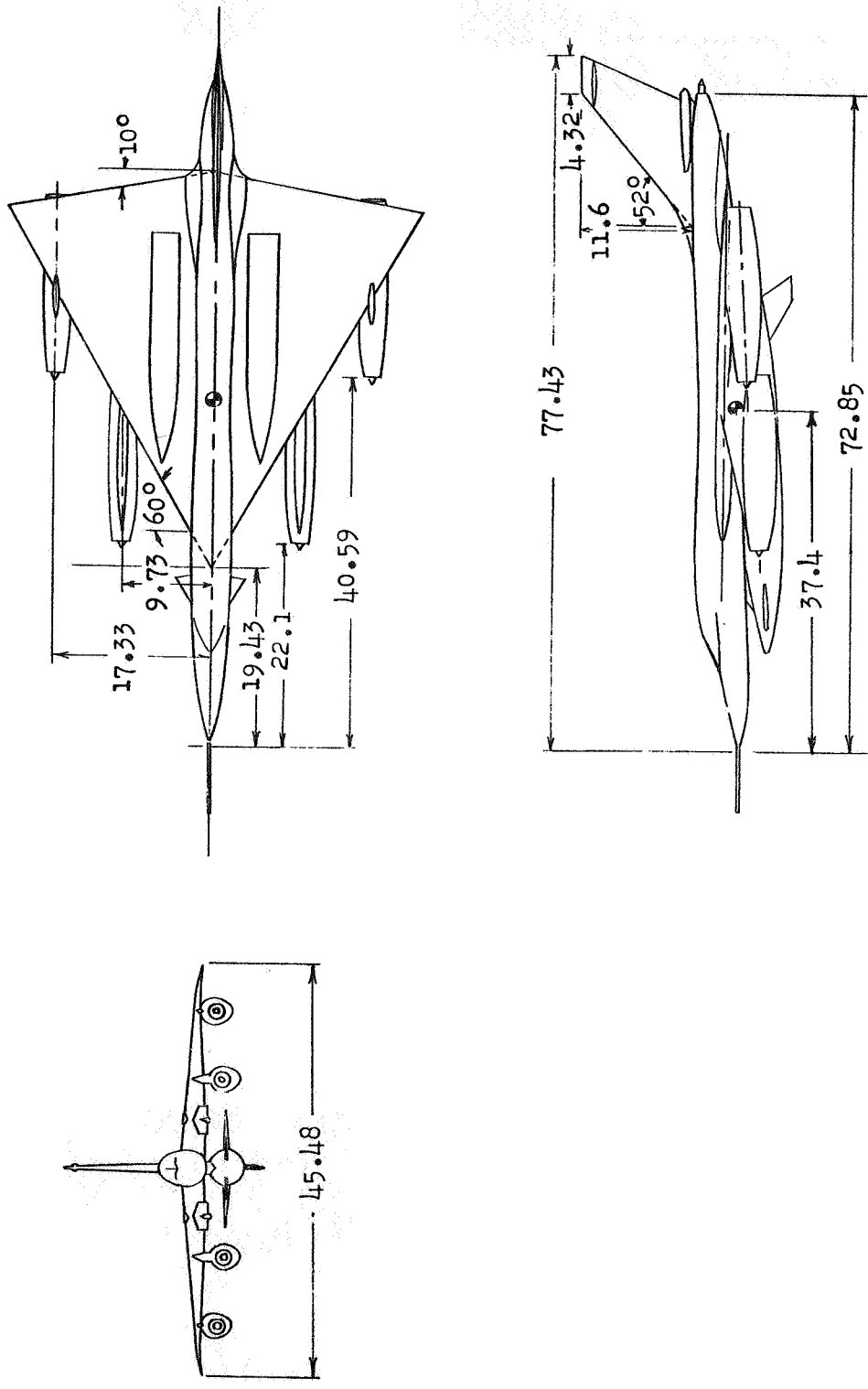
Area (included), sq in.	89.60
Span, in.	13.70
Aspect ratio	2.10
Airfoil section	NACA 0004.5-64

Pod canard:

Area (included), sq in.	29.44
Span, in.	7.86
Aspect ratio	2.10
Airfoil section	NACA 0004.5-64

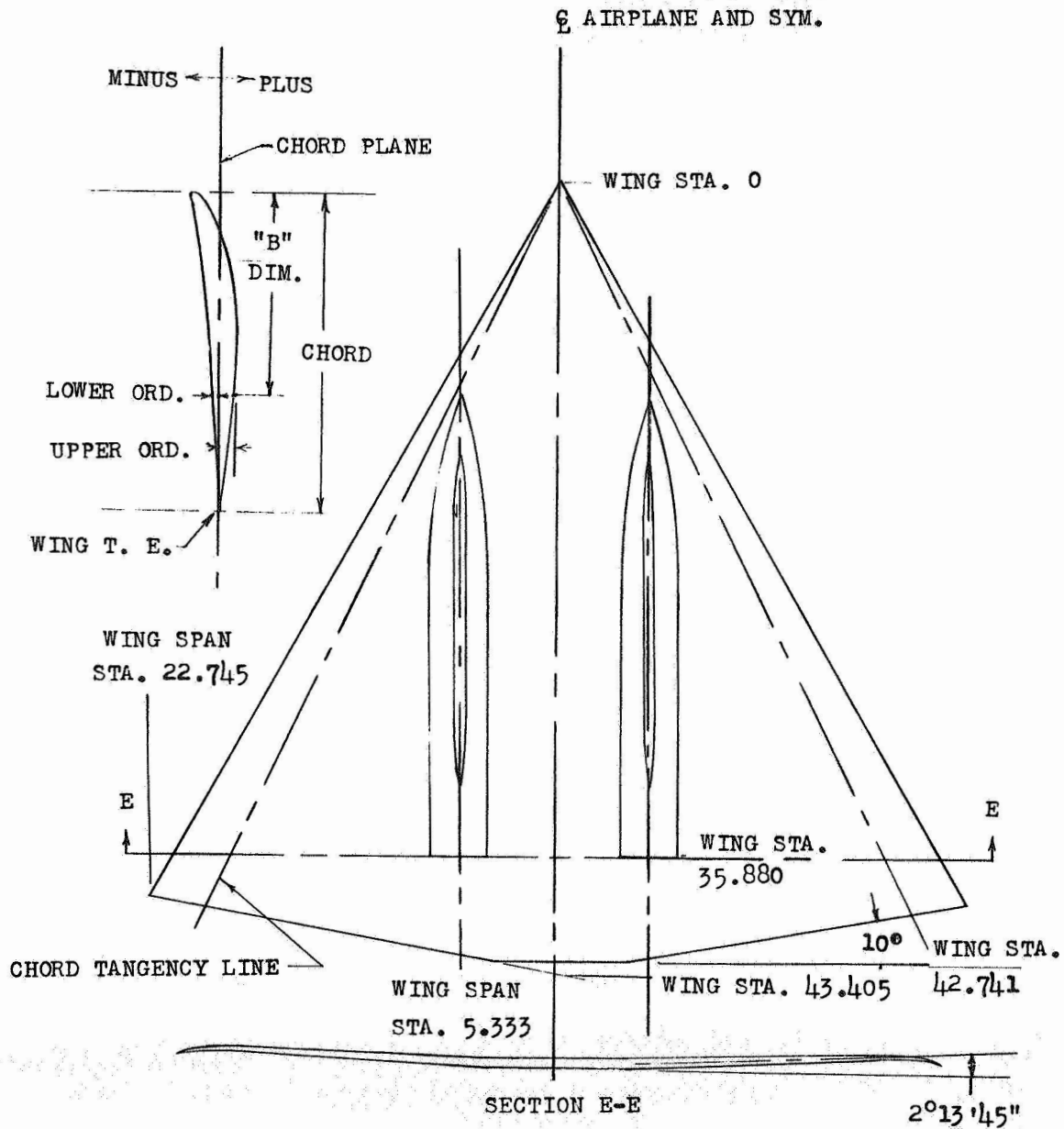
Pod ventral fin:

Area (included), sq in.	19.20
Span, in.	4.10
Aspect ratio	1.75
Taper ratio	0.35
Airfoil section	NACA 0004.5-64
Leading-edge sweep	60



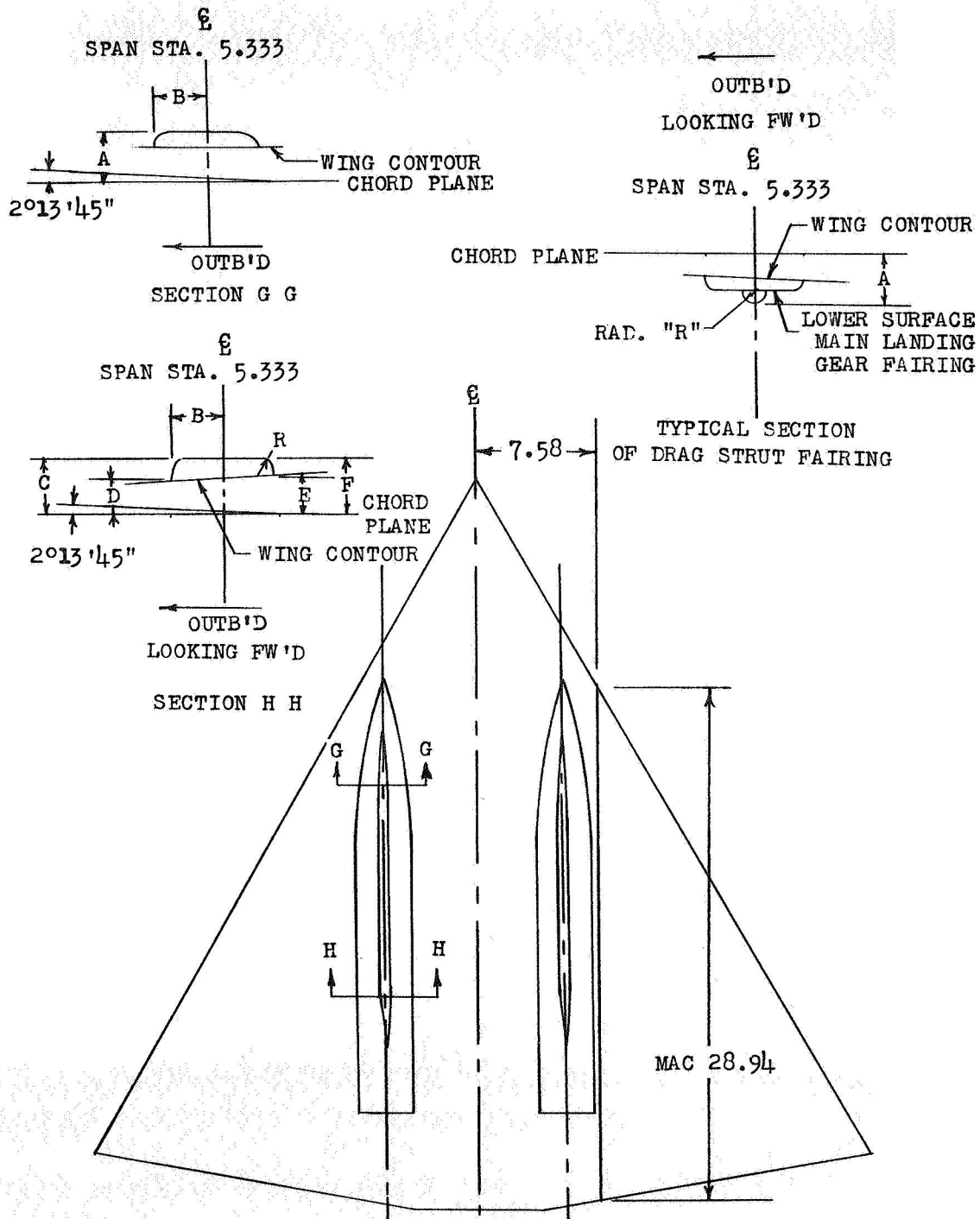
(a) Sketch of complete model.

Figure 1.- General arrangement of model. All dimensions are in inches.



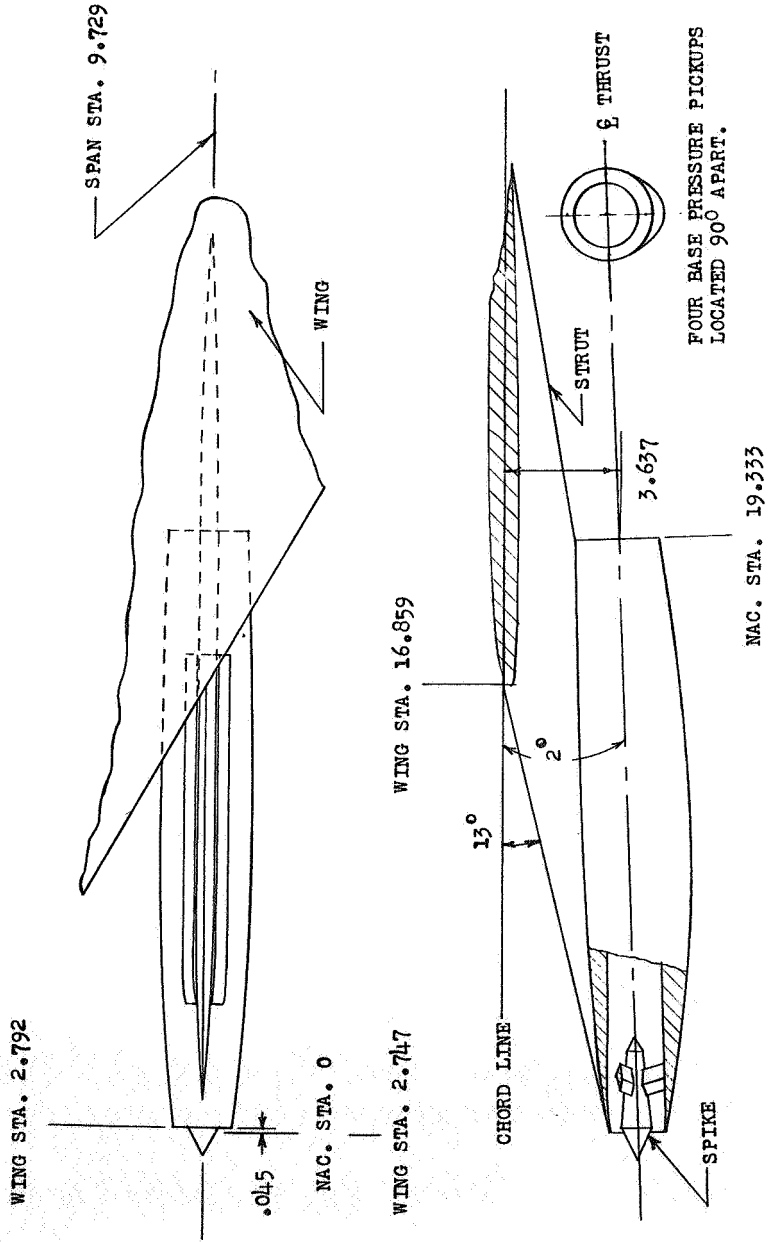
(b) Wing geometry. (Also, see table I.)

Figure 1.- Continued.



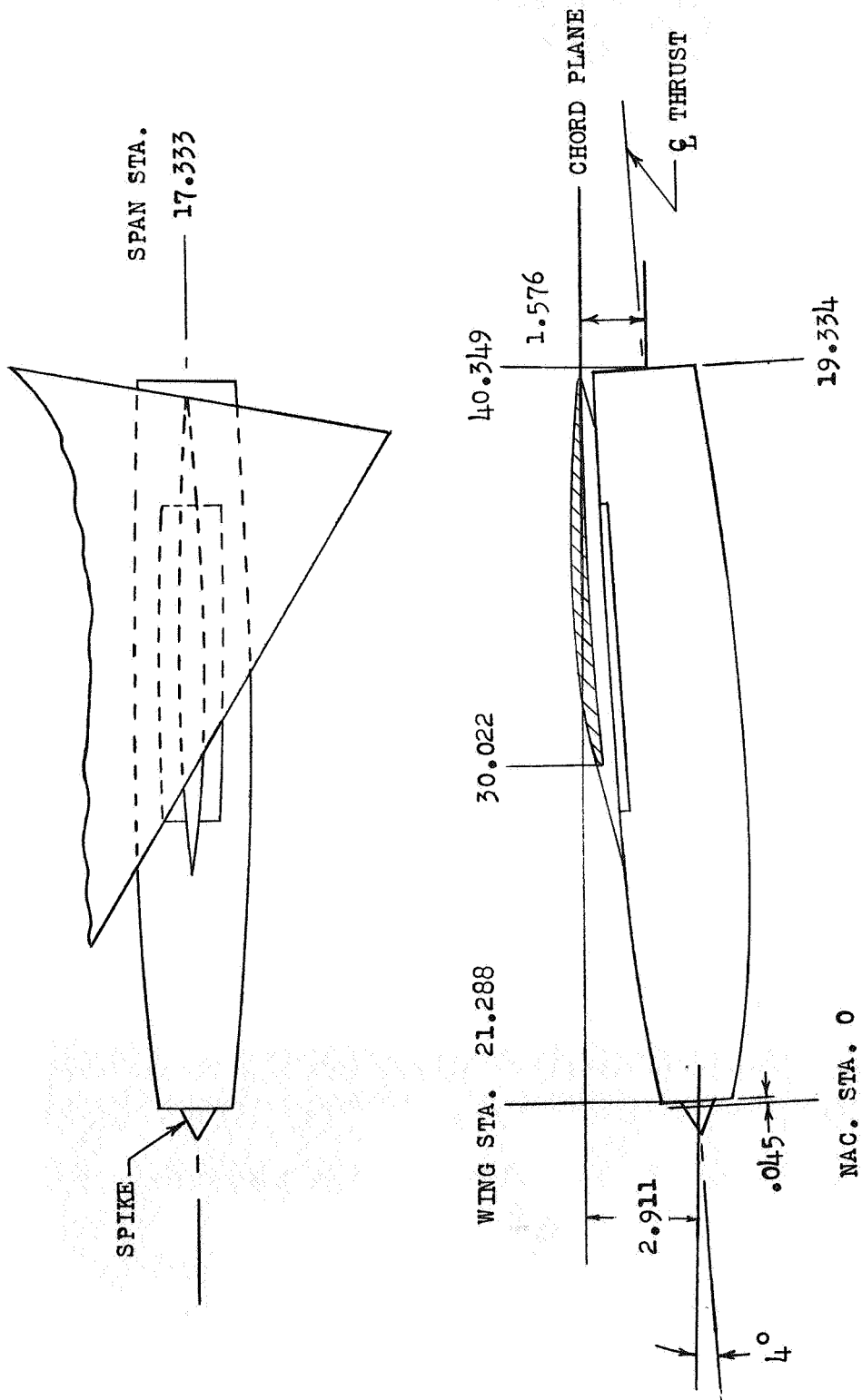
(c) Detail of drag strut fairing and main landing-gear fairing.

Figure 1.- Continued.



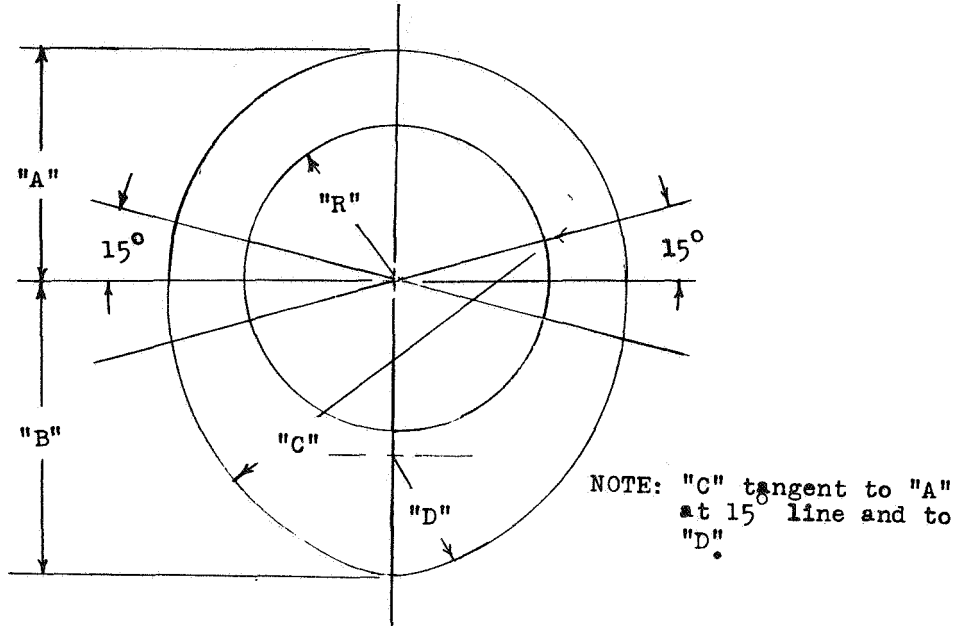
(d) Inboard engine nacelle and strut.

Figure 1.- Continued.



(e) Outboard engine nacelle and strut.

Figure 1.- Continued.

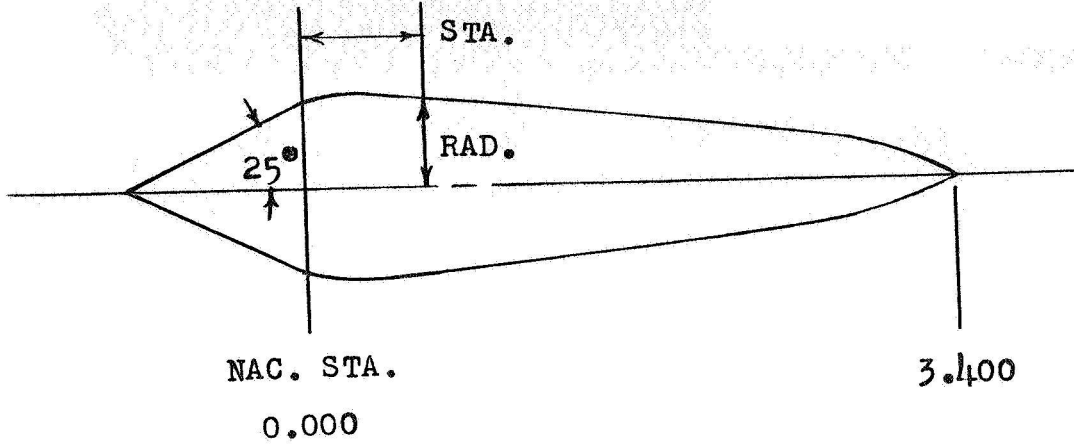


NACELLE GEOMETRY			
STA.	"A"	"B"	"D"
.124	.997	.997	-
.134	1.007	1.007	.800
.149	1.015	1.015	
.170	1.019	1.019	
.184	-	-	
.197	-	-	
.333	1.049	1.052	
.453	-	-	
.666	1.100	1.115	
1.333	1.172	1.242	
2.000	1.219	1.360	
2.666	1.254	1.475	
4.000	1.307	1.669	
6.000	1.381	1.869	
8.000	1.447	1.966	
10.000	1.487	1.971	
10.666	1.491	1.961	
12.000	1.486	1.919	
14.000	1.449	1.802	
16.000	1.399	1.621	
18.000	1.369	1.455	
18.666	1.367	1.409	
19.333	1.367	1.367	.800

NAC. INTERNAL GEOMETRY	
STA.	"R"
.124	.997
.134	.987
.149	.982
.170	.980
.184	.979
.197	.979
.453	.985
15.866	.985
18.667	.878
19.333	.845

(f) Nacelle geometry.

Figure 1.- Continued.

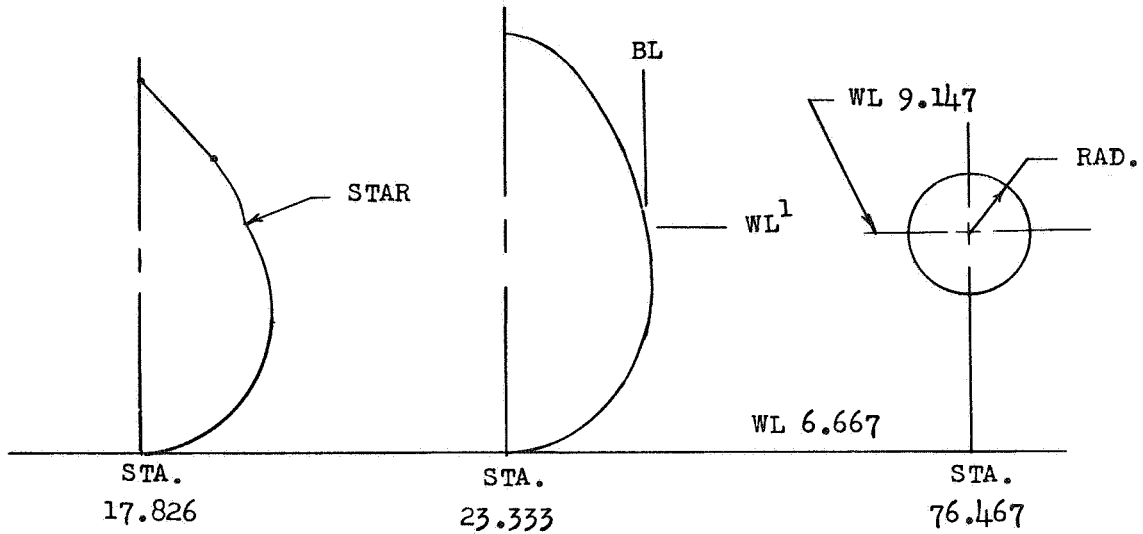


SPIKE GEOMETRY

NAC. STA.	RAD.
-.955	0
0	.445
.113	.474
.227	.486
.340	.478
.453	.469
.567	.458
1.133	.399
1.700	.342
2.267	.283
2.833	.214
2.947	.181
3.060	.136
3.173	.091
3.287	.045
3.400	0

(g) Engine nacelle spike.

Figure 1.- Continued.



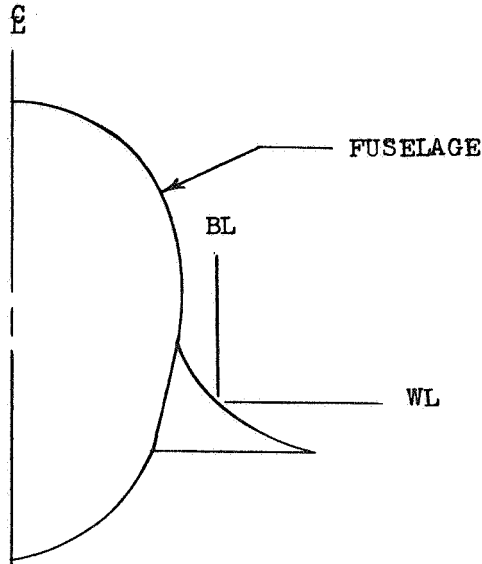
* STRAIGHT LINE BETWEEN ORDINATES BEARING THIS SYMBOL

STA. 0		STA. 1.00		STA. 6.000		STA. 10.000		STA. 12.159	
WL ¹	BL	WL ¹	L	L ¹	BL	WL ¹	BL	WL ¹	BL
1.042	0	.877	0	0	0	0	0	0	0
		.917	.167	.217	.0	.083	.803	.083	.930
		1.000	.253	.250	.617	.167	1.052	.167	1.173
		1.083	.261	.333	.893	.250	1.230	.250	1.343
		1.167	.225	.417	1.023	.333	1.350	.333	1.453
		1.250	.120	.500	1.107	.500	1.527	.500	1.620
		1.273	0	.667	1.213	.667	1.633	.667	1.723
				1.000	1.340	1.000	1.759	1.000	1.850
				1.333	1.370	1.333	1.805	1.333	1.907
				1.667	1.297	1.667	1.802	1.667	1.920
				2.000	1.090	2.000	1.781	2.000	1.903
				2.167	.867	2.333	1.650	2.333	1.852
				2.333	.420	2.667	1.411	2.667	1.748
				2.380	0	3.000	.887	2.897	1.608
						3.108	.450	3.000	1.78
						3.140	0	3.333	1.017
						3.483	0	3.633	1.37
								4.543	0.083
									0

¹WL is distance above WL 6.667 ,

(h) Fuselage geometry.

Figure 1.- Continued.



STA. 50.000		STA. 53.333		STA. 56.667		STA. 60.000		STA. 64.133	
WL ¹	BL	WL ¹	BL	WL ¹	BL	WL ¹	L	WL ¹	BL
1.647	1.369	1.377	1.547	1.085	2.045	.777	2.732	.590	3.278
		1.417	1.427	1.167	1.755	.833	2.425	.667	2.788
		1.500	1.347	1.250	1.641	1.000	2.127	.833	2.437
		1.611	1.324	1.333	1.567	1.167	1.937	1.000	2.202
				1.500	1.459	1.333	1.789	1.333	1.872
				1.667	1.395	1.500	1.673	1.667	1.648
				1.885	1.355	1.667	1.575	2.000	1.510
						2.000	1.445	2.333	1.425
						2.233	1.393		

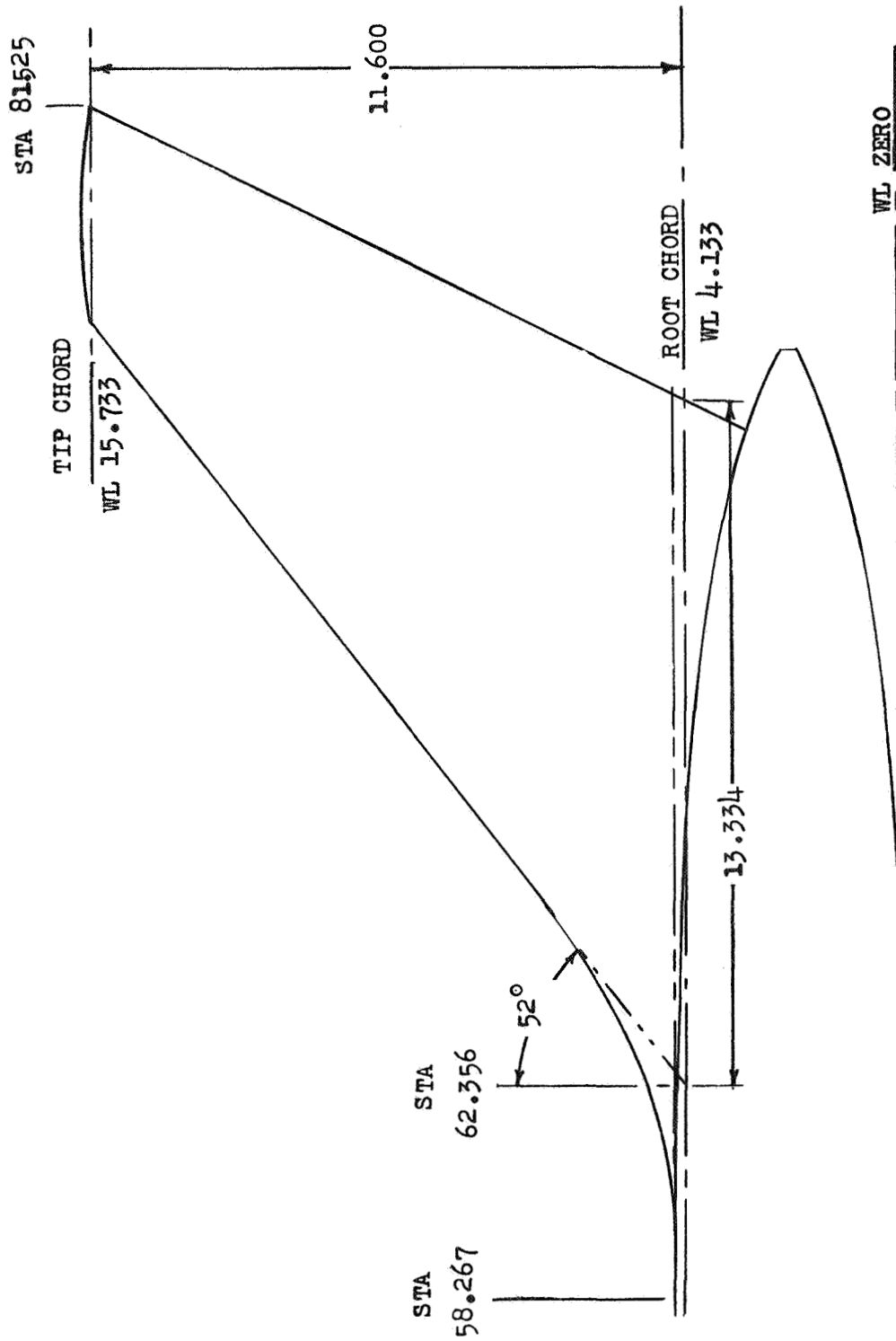
STA. 67.467		STA. 70.800		STA. 72.000		STA. 72.667		STA. 73.333	
WL ¹	BL	WL ¹	BL	WL ¹	BL	WL ¹	BL	WL ¹	BL
.520	2.207	.790	.873	1.103	.455	1.067	.227	1.223	0
.540	2.207	.803	.873	1.167	.500	1.160	.380		
.583	2.060	.833	.850	1.203	.753				
.667	1.963	1.000	.919						
.750	1.883	1.167	.987						
.833	1.823	1.443	1.113						
1.000	1.713								
1.333	1.567								
1.667	1.463								
2.113	1.419								

¹WL is distance above WL 6.667

(i) Fuselage-wing fillet geometry.

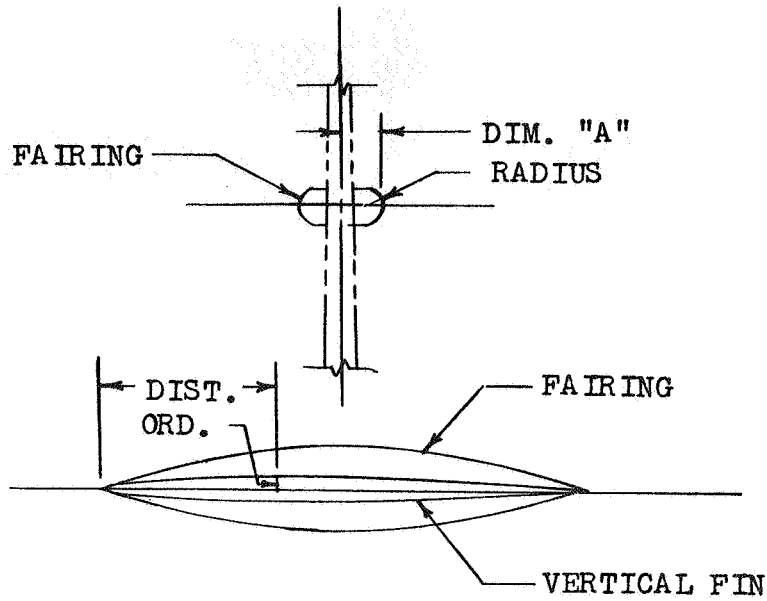
Figure 1.- Continued.





(j) Vertical fin.
Figure 1.- Continued.

SECRET



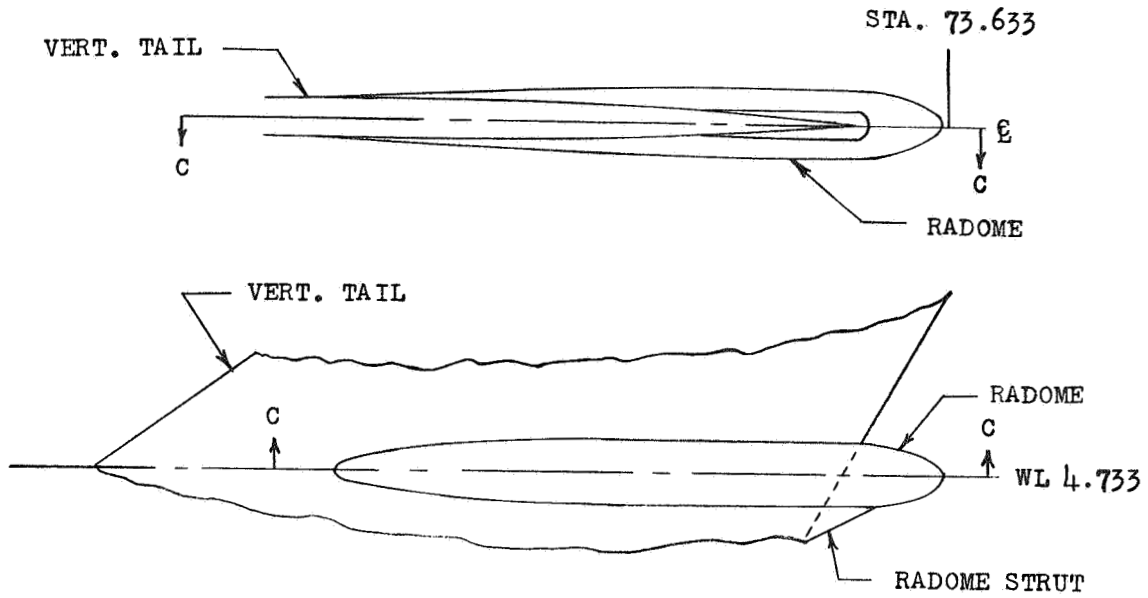
ACTUATOR FAIRING SECTIONS				
STA.	Span Station 7.918			
	Dist.	Dim A	Radius	FinOrd
0	0	-	-	0
1.25	.075	-	-	.045
2.06	.123	.054	0	-
2.50	.148	-	-	.060
5	.298	.097	.022	.081
10	.595	.163	.062	.105
20	1.191	.282	.130	.132
30	1.786	.375	.176	.145
40	2.382	.437	.198	.148
50	2.977	.461	.199	.145
60	3.571	.443	.185	.132
70	4.167	.389	.155	.111
80	4.762	.287	.111	.082
90	5.358	.151	.059	.047
95	5.655	.082	.031	.025
100	5.953	0	0	0

(k) Actuator fairing.

Figure 1.- Continued.



RADOME GEOMETRY

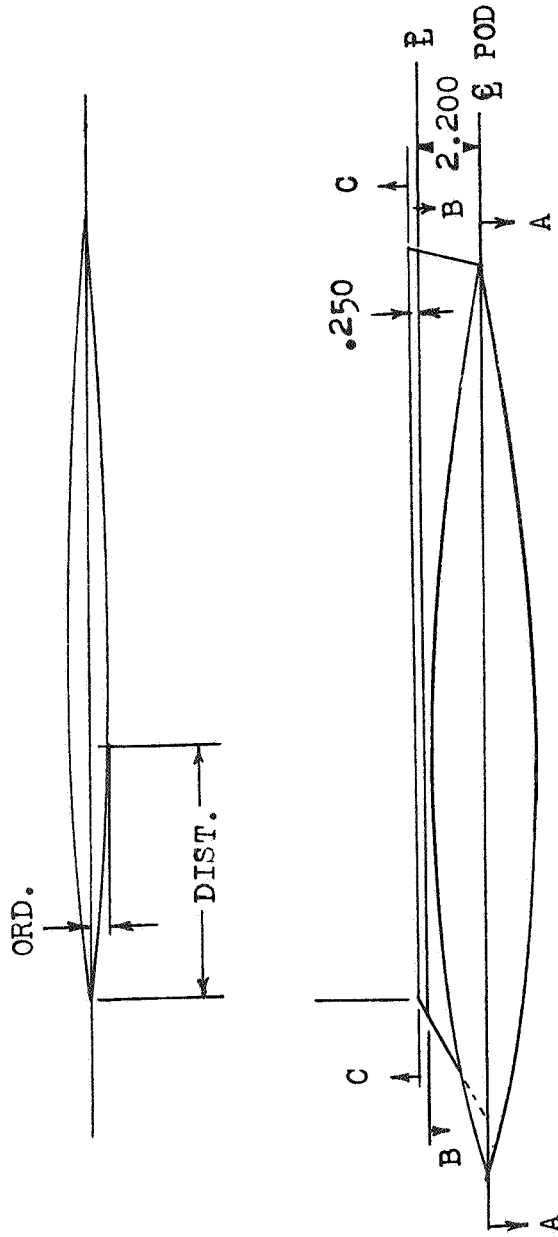


RADOME GEOMETRY	
STA.	ORD.
63.100	.316
64.214	.408
65.911	.500
67.233	.534
72.417	.534
72.617	.529
72.817	.498
73.217	.357
73.416	.260
73.633	.000

(1) Radome geometry.

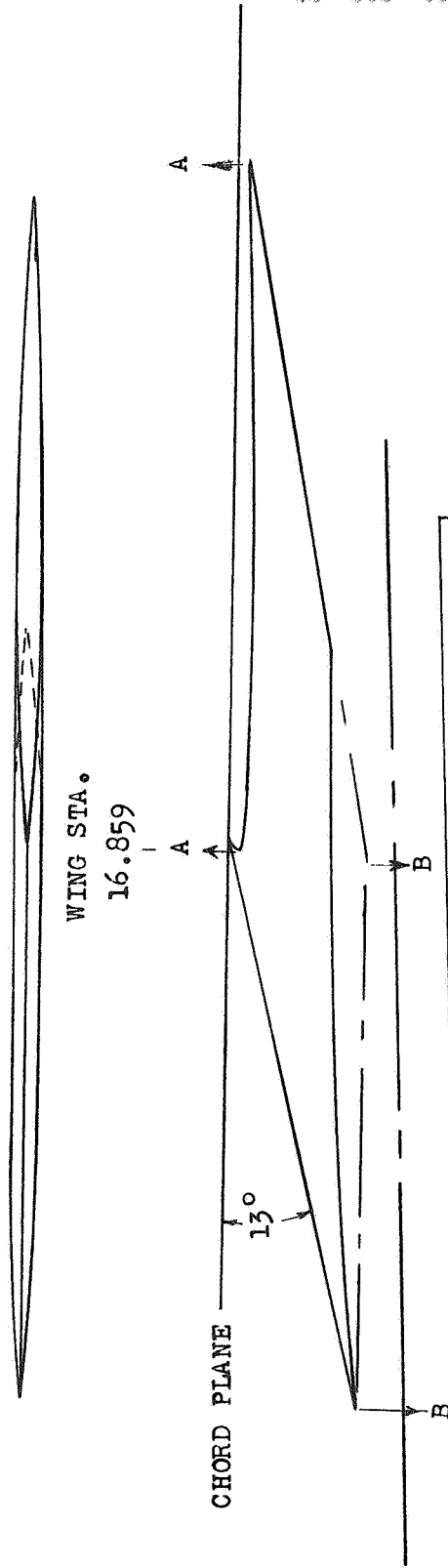
Figure 1.- Continued.





(m) Pod and pod strut geometry.

Figure 1.- Continued.

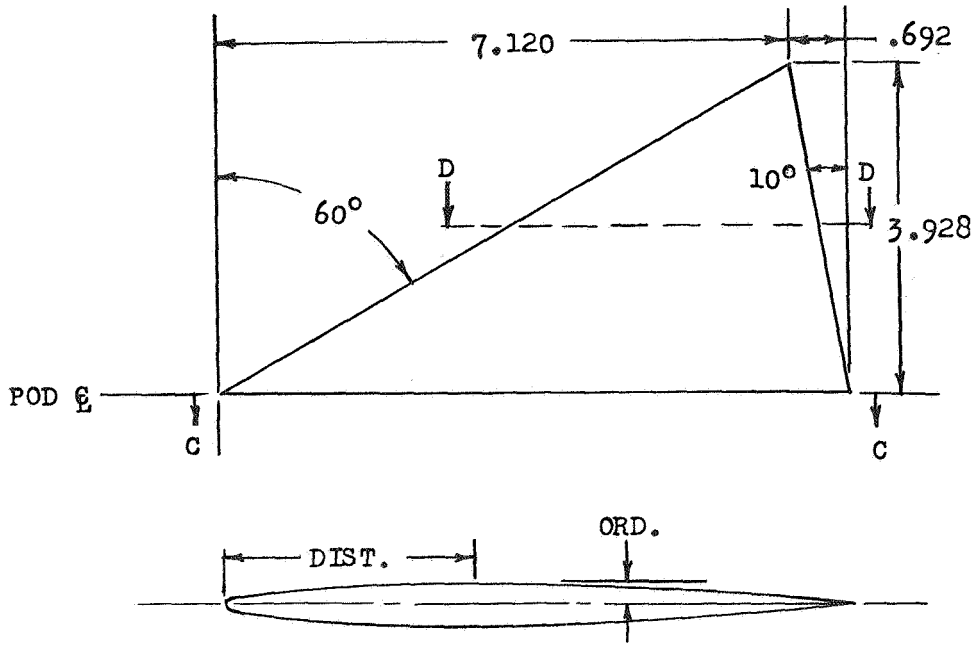


STRUT GEOMETRY			
SECT. A-A		SECT. B-B	
DIST.	ORD.	DIST.	ORD.
0	.005R	0	.005R
.915	.151	.634	.105
1.830	.259	1.268	.179
3.660	.393	2.536	.273
5.489	.447	3.805	.310
7.320	.457	5.073	.317
9.149	.444	6.341	.308
10.978	.405	7.609	.281
12.809	.341	8.877	.236
14.638	.253	10.146	.176
16.468	.112	11.414	.099
17.383	.078	12.048	.054
18.298	.005R	12.682	.005R

(n) Strut geometry.

Figure 1.- Continued.

POD STA. 2.120



TYPICAL SECTION NACA 0004.5-64

CANARD AT ZERO INCIDENCE AND DIHEDRAL
 ROOT CHORD 2.200 INCHES BELOW PARTING
 PLANE NACA 0004.5-64 AIRFOIL SECTION

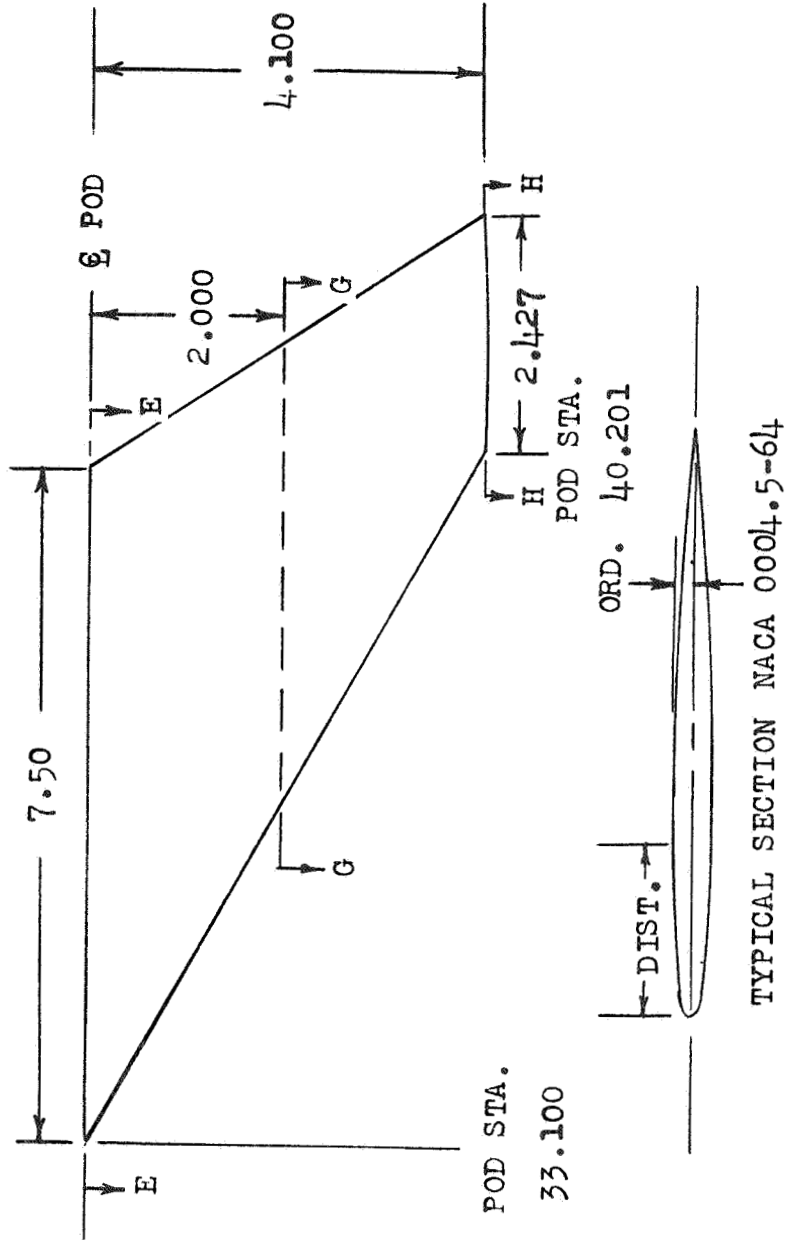
CHORD	SECTION C-C		SECTION D-D	
	DIST.	ORD.	DIST.	ORD.
0	0	0	0	0
5	.375	.092	.184	.045
10	.750	.119	.368	.058
15	1.124	.137	.552	.067
20	1.499	.149	.736	.073
30	2.248	.164	1.104	.080
40	2.998	.169	1.472	.083
50	3.748	.1644	1.840	.080
60	4.497	.149	2.207	.073
70	5.247	.126	2.575	.062
80	5.996	.093	2.943	.046
90	6.746	.053	3.311	.026
95	7.120	.029	3.495	.014
100	7.495	.0	3.679	0
	L.E.R	.015	L.E.R	.007

(o) Pod canard geometry.

Figure 1.- Continued.

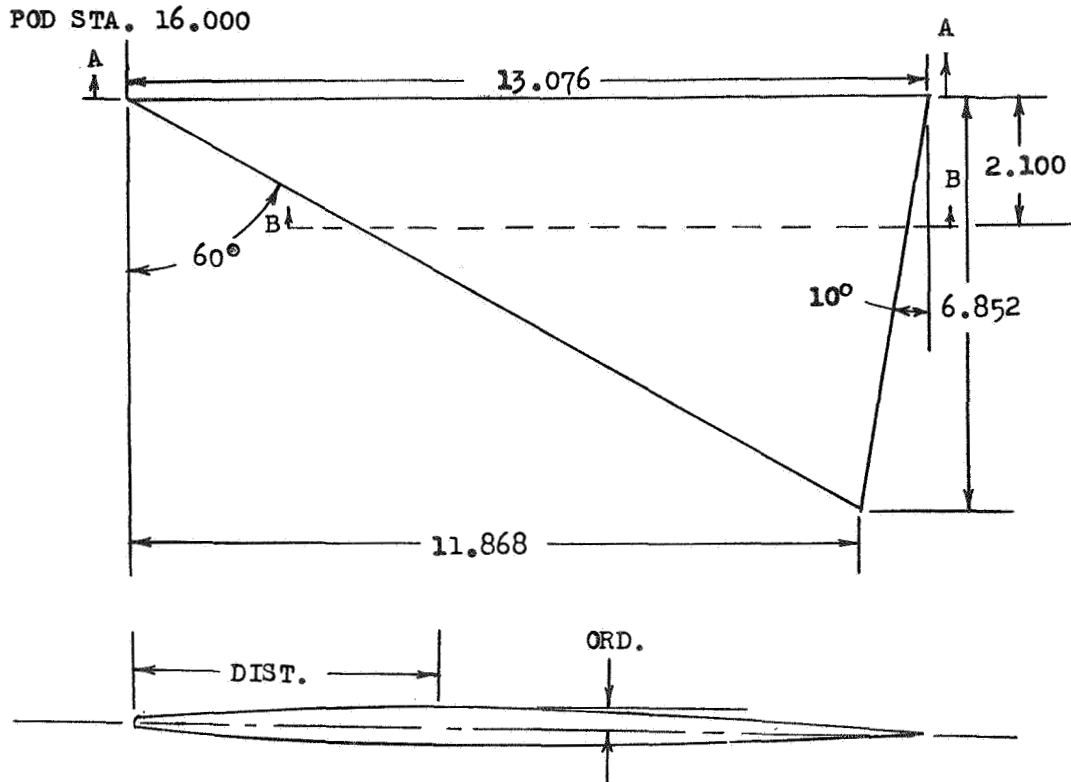


SECRET



(p) Pod ventral fin.

Figure 1.- Continued.



TYPICAL SECTION NACA 0004.5-64

Pod Wing Geometry				
Chord	Sect. A-A		Sect. B-B	
	Dist.	Ord.	Dist.	Ord.
0	0	0	0	0
5	.653	.160	.453	.111
10	1.308	.208	.907	.144
15	1.961	.238	1.360	.165
20	2.615	.260	1.814	.180
30	3.923	.286	2.721	.198
40	5.230	.294	3.628	.204
50	6.538	.286	4.535	.198
60	7.846	.261	5.441	.181
70	9.153	.220	6.348	.152
80	10.461	.163	7.255	.113
90	11.768	.092	8.162	.064
95	12.422	.050	8.616	.035
100	13.076	0	9.069	0
LER		.029		.020

(q) Pod wing geometry.

Figure 1.- Concluded.



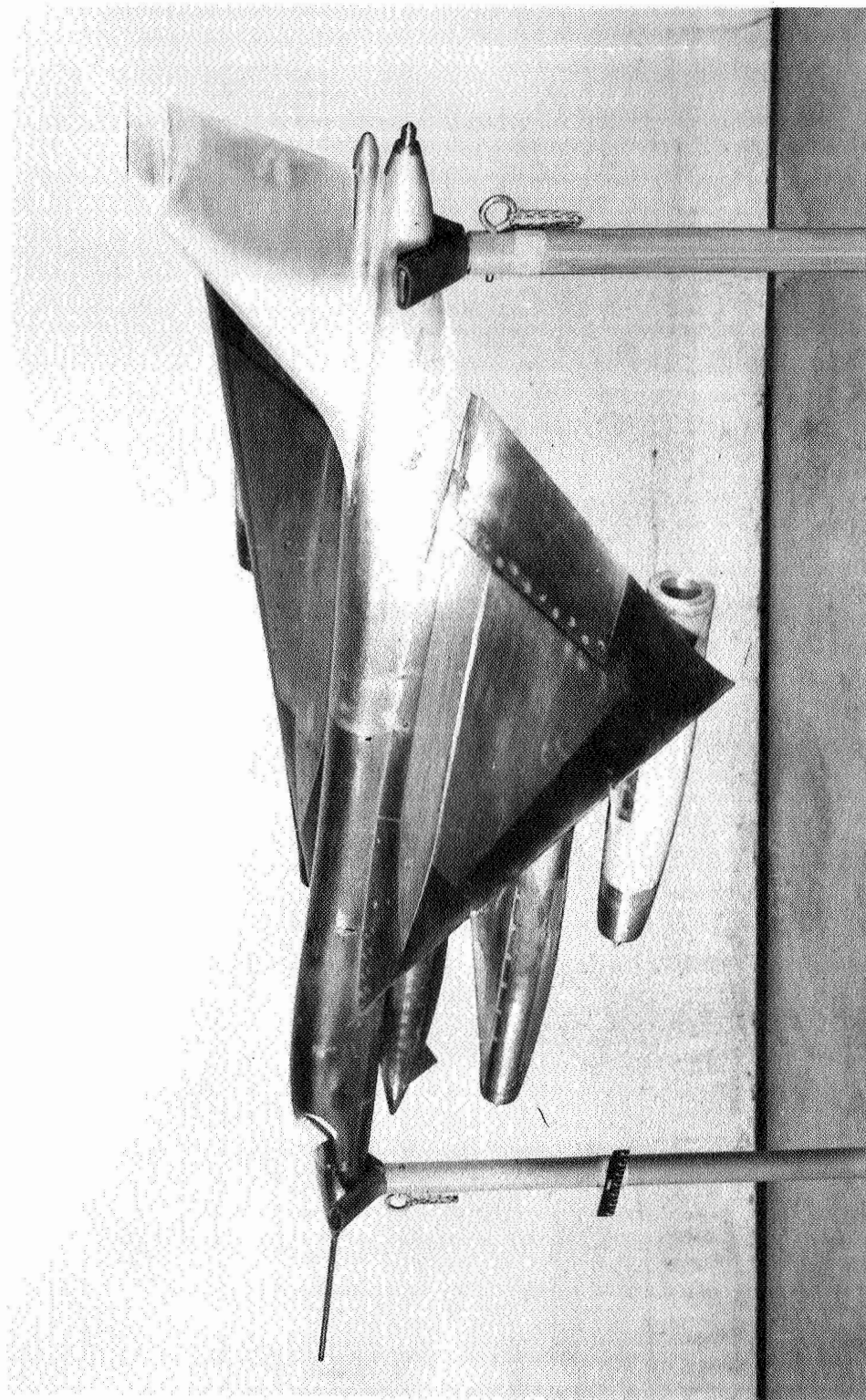
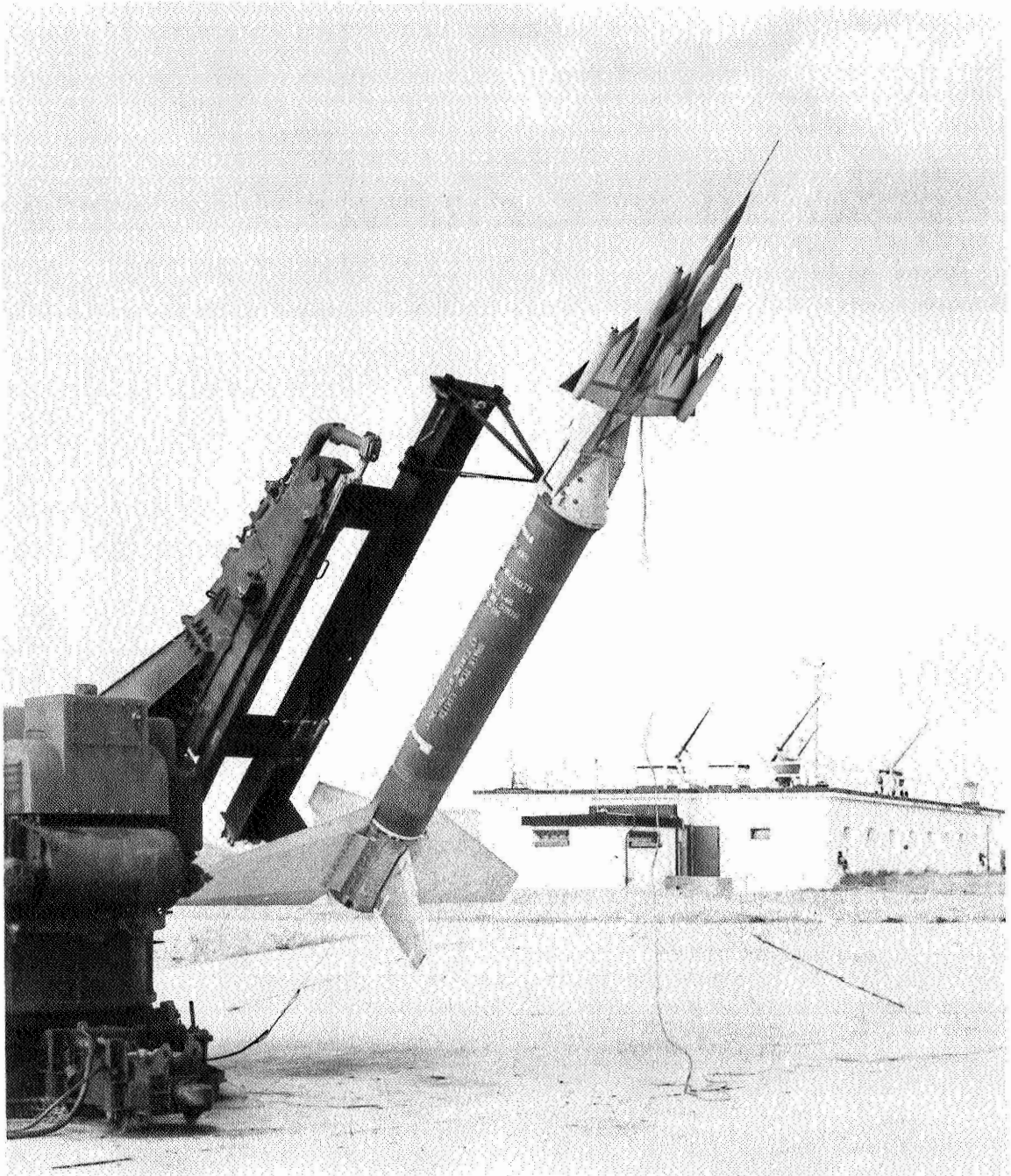


Figure 2.- Photograph of model. L-91949.1



L-92185.1

Figure 3.- Model and booster in launch position.



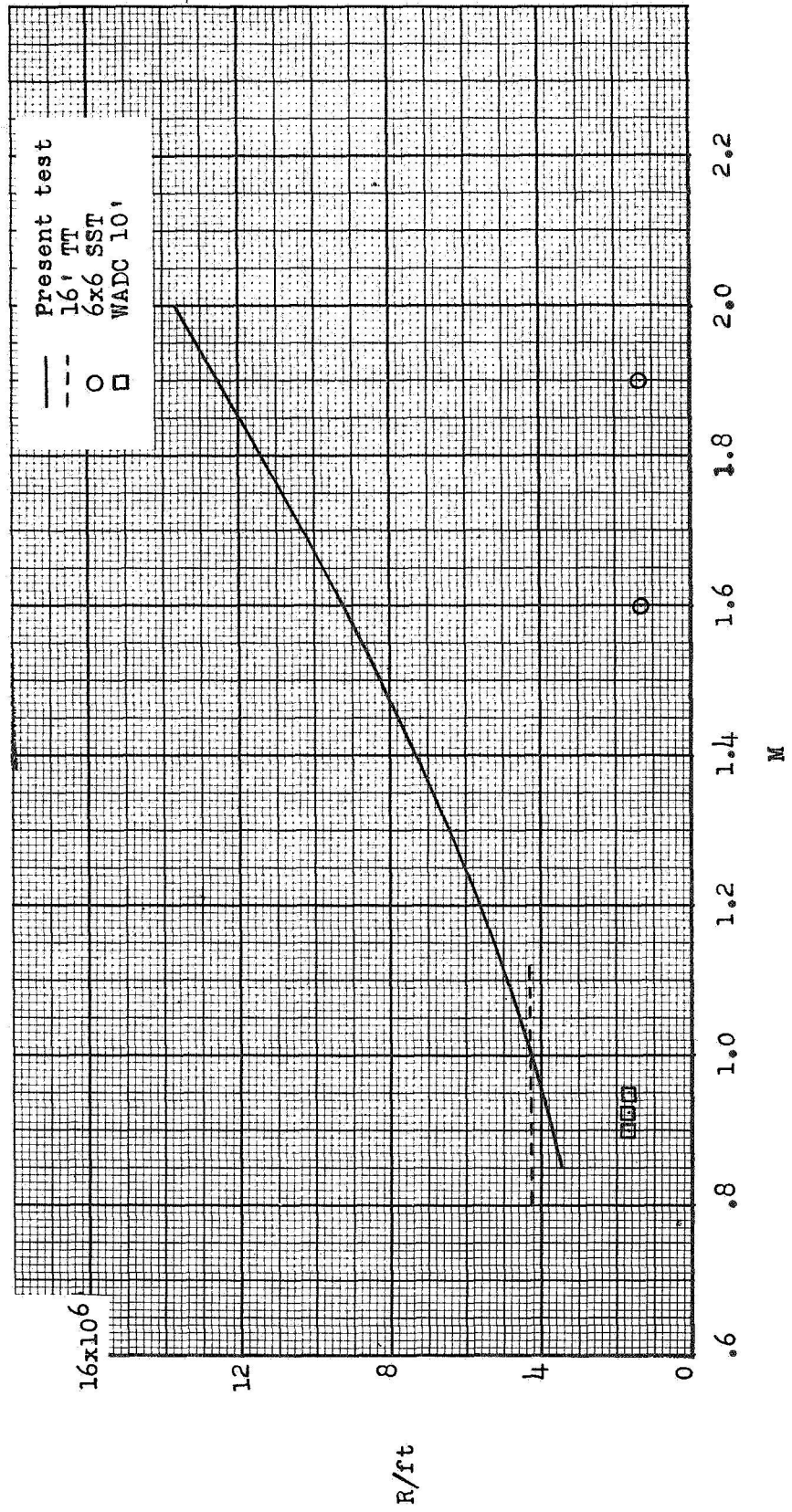


Figure 4.- Variation of Reynolds number with Mach number.

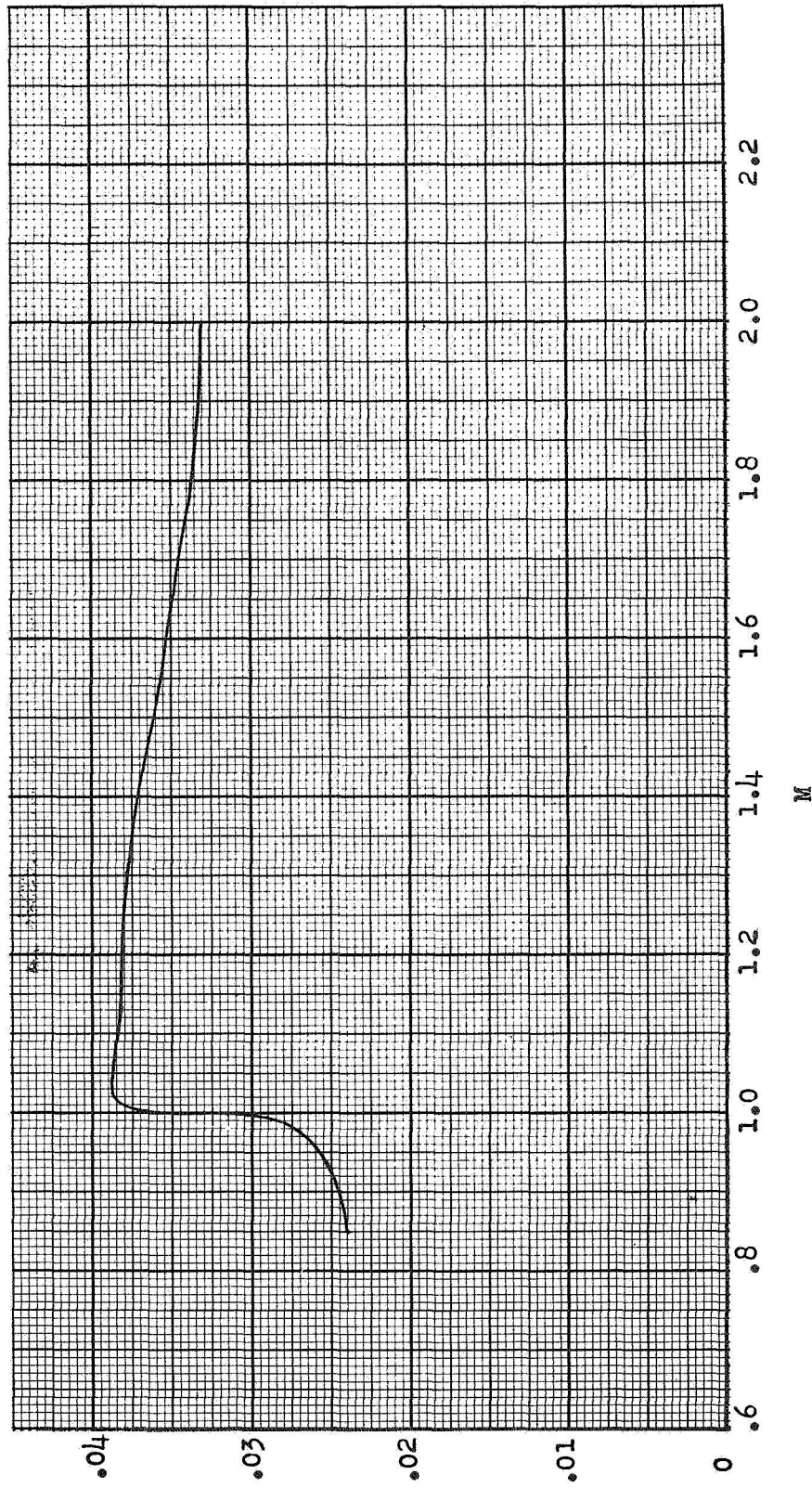


Figure 5.-- Total drag.

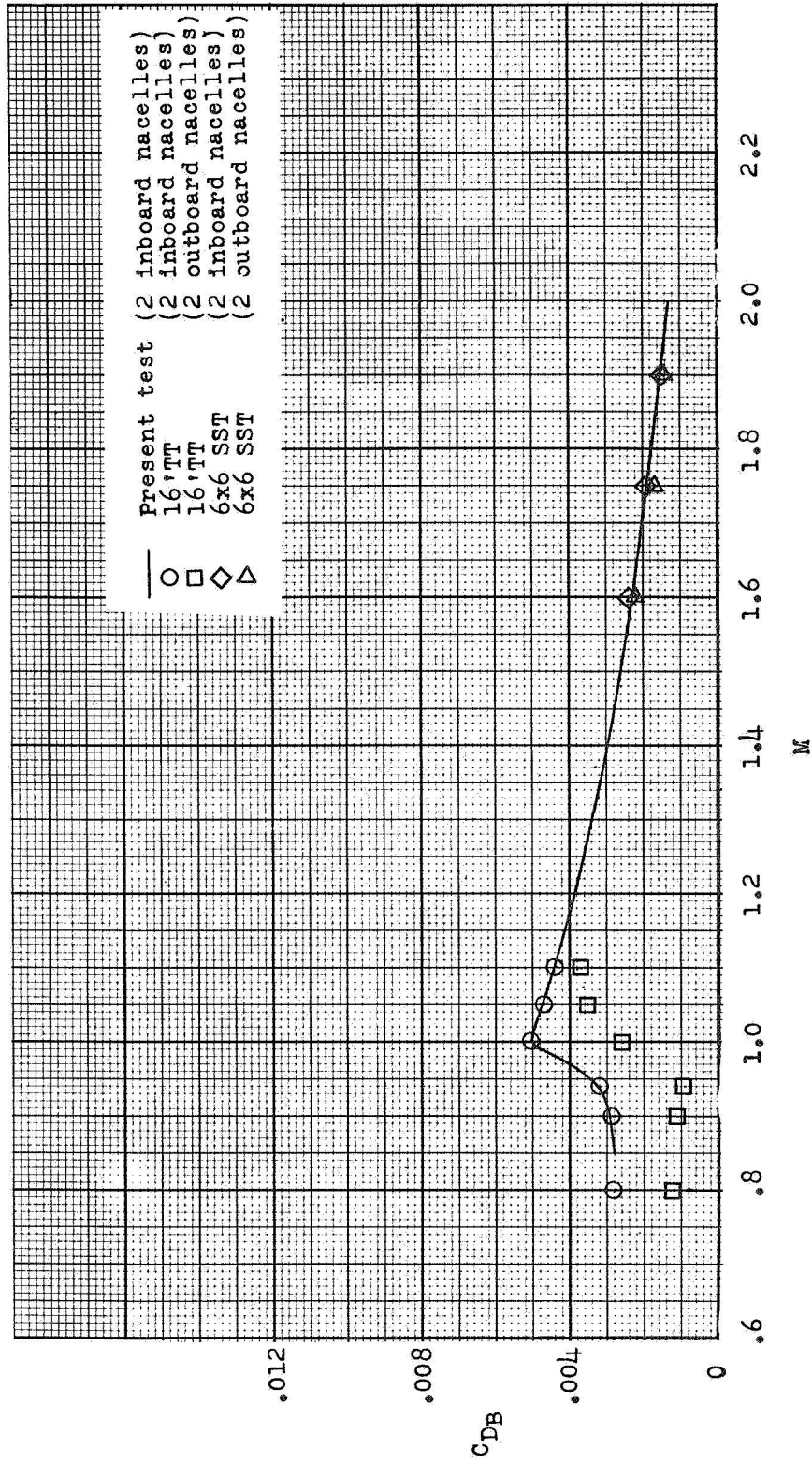


Figure 6.- Base drag.

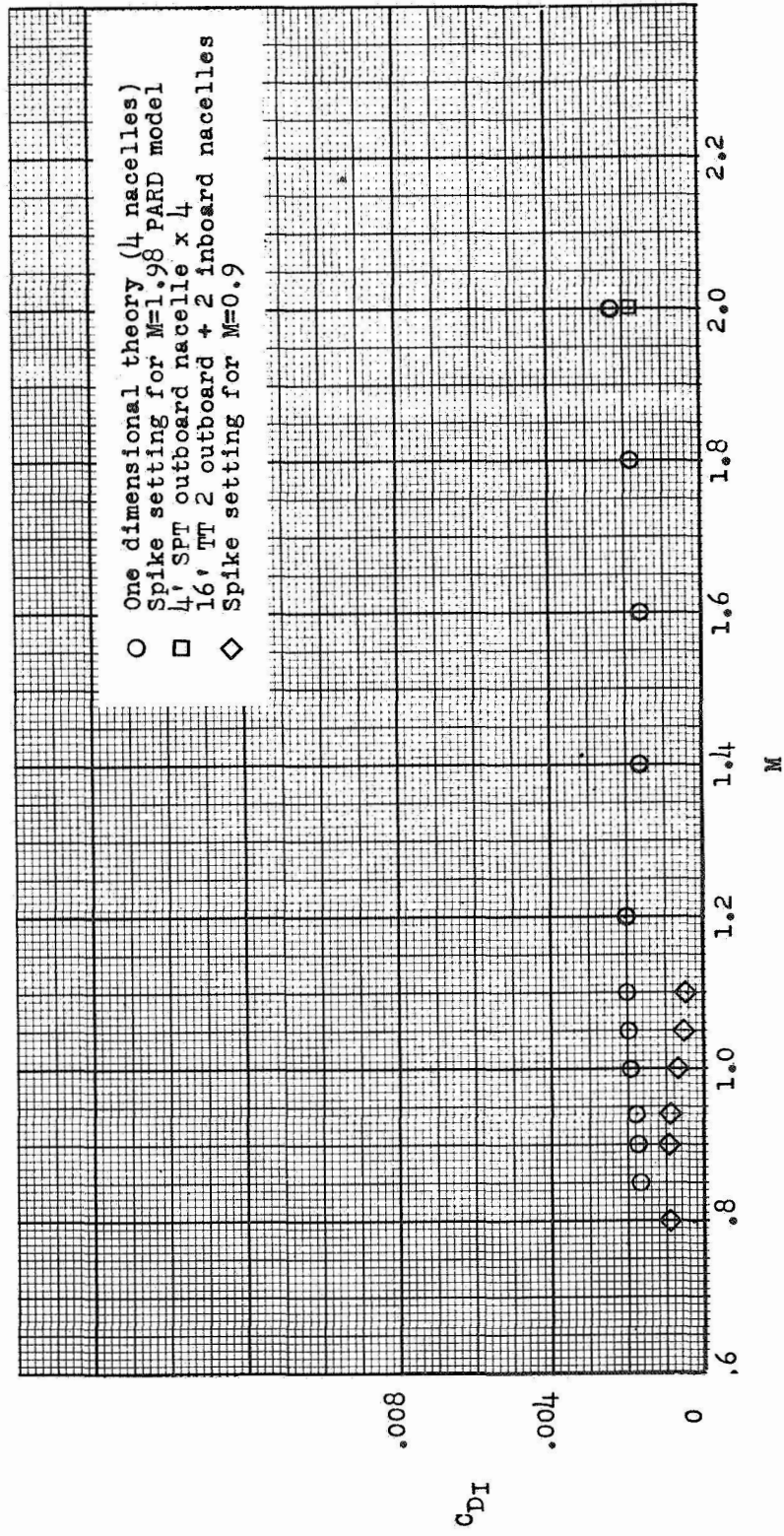


Figure 7.- Internal drag.

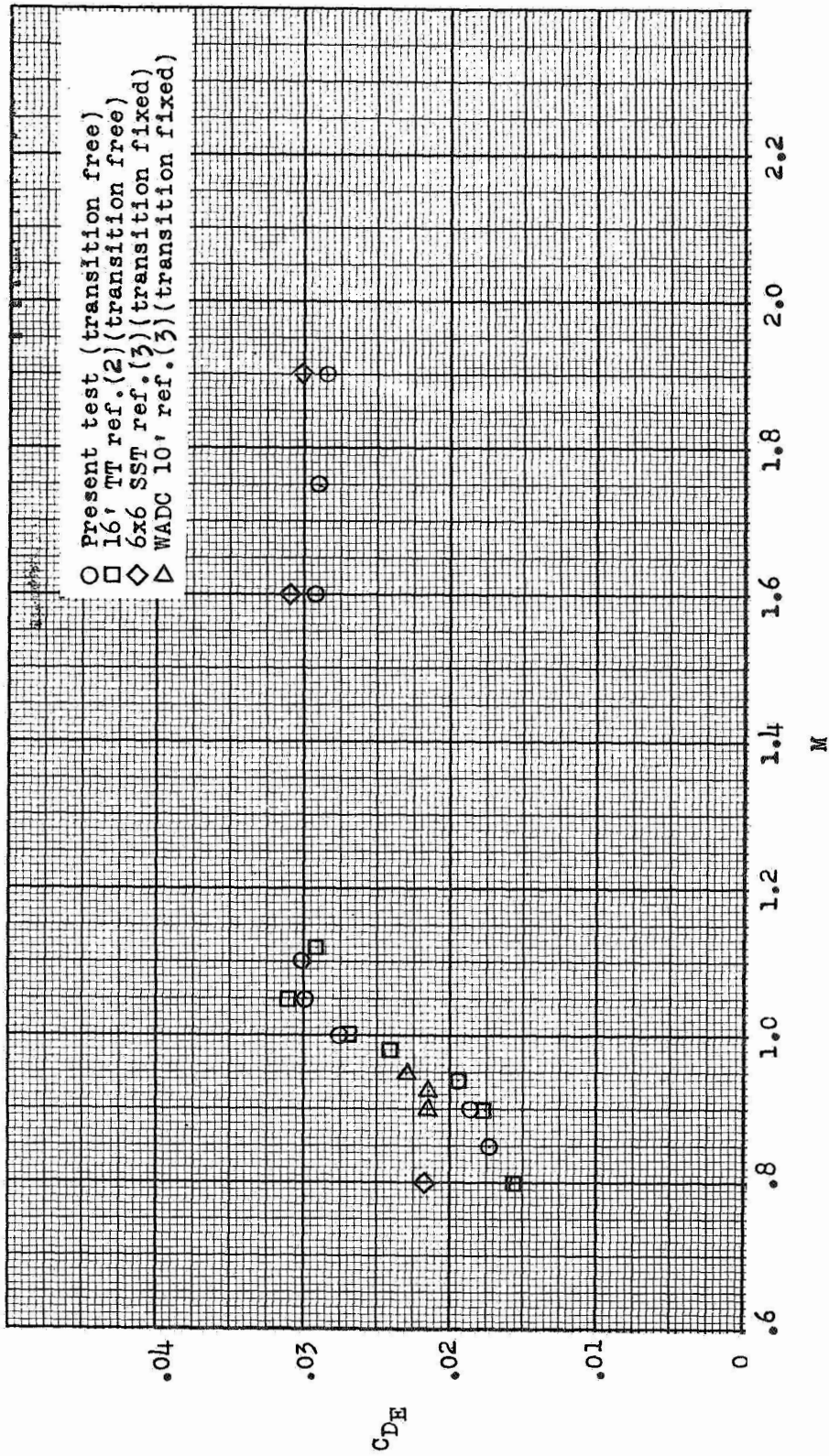


Figure 8.- Comparison of external drag data at model flight C_n.

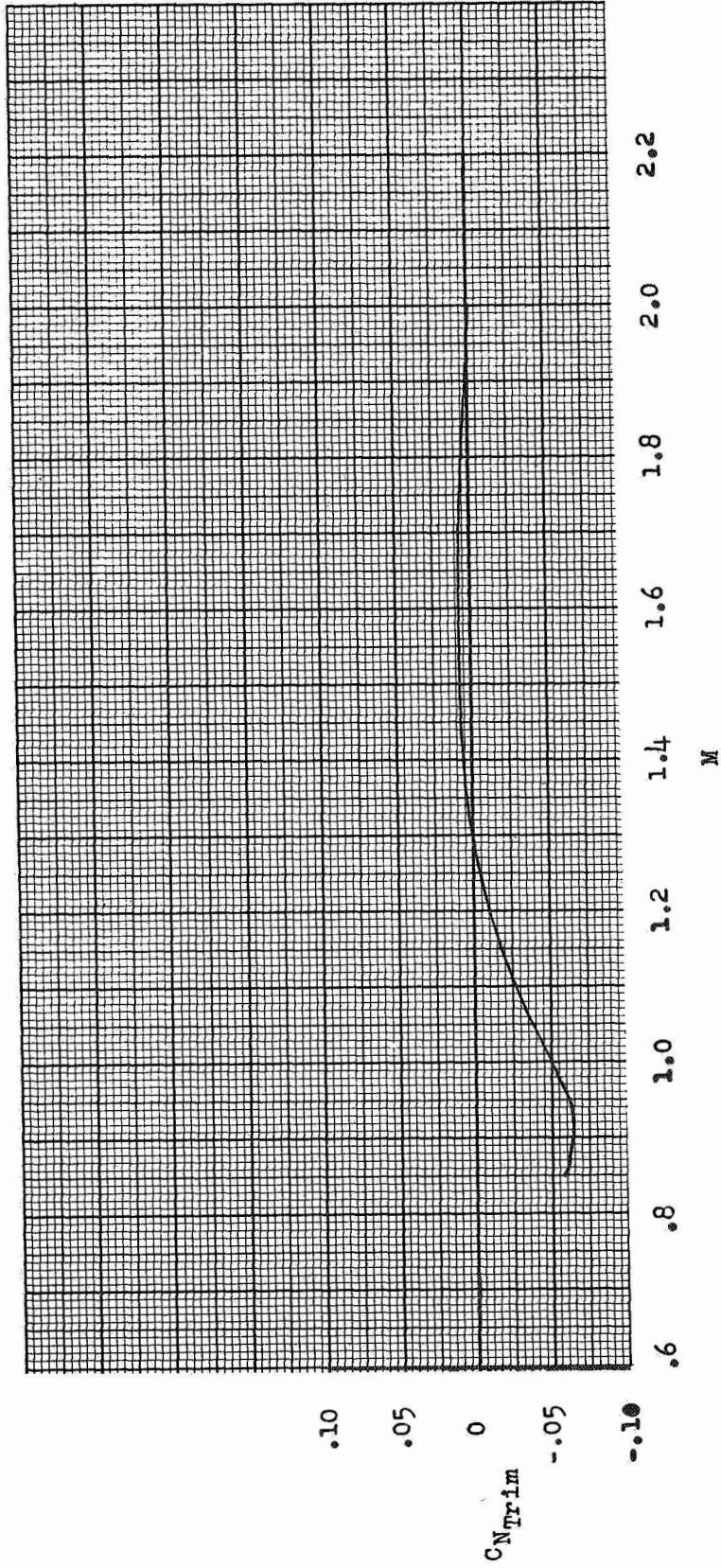


Figure 9.- Trim normal force. Center of gravity at station 37.4.

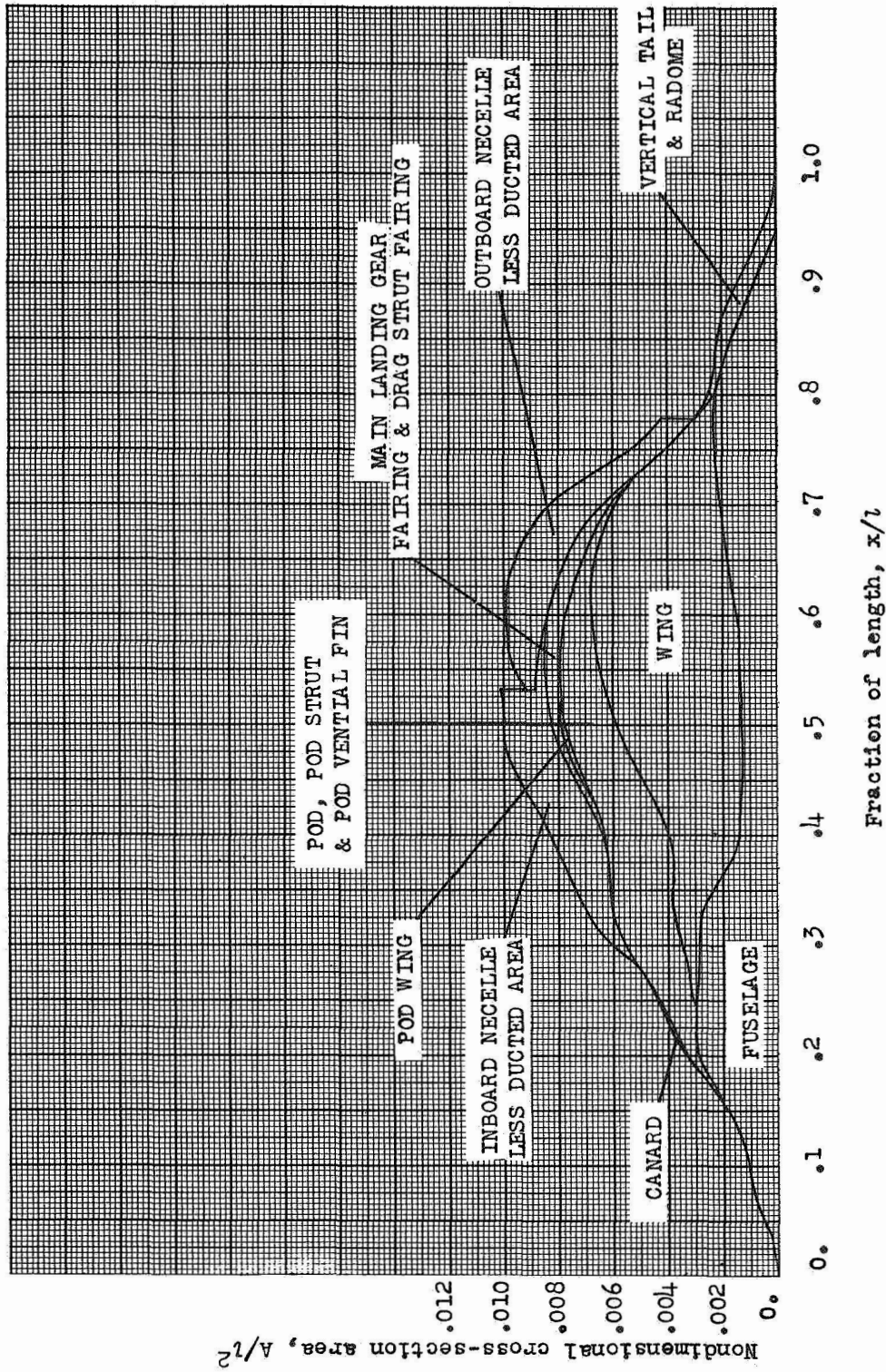


Figure 10.- Nondimensional cross-sectional area distribution.

INDEX

<u>Subject</u>	<u>Number</u>
Airplanes - Specific Types	1.7.1.2
Airplanes - Performance	1.7.1.3

ABSTRACT

An investigation has been made by the Langley Pilotless Aircraft Research Division utilizing a 1/15-scale rocket-propelled model of the Convair B-58 supersonic bomber. The drag at model trim lift was obtained at Mach numbers between 0.85 and 2.0 at corresponding Reynolds number per foot of 3.5×10^6 and 13.7×10^6 , respectively. The results of the present investigation are compared with unpublished data obtained from several facilities, WADC 10-foot tunnel, Ames 6- by 6-foot supersonic tunnel and the Langley 16-foot transonic tunnel. A comparison of the drag at transonic speeds and at approximately the same Reynolds numbers showed excellent agreement. A drag coefficient of 0.028 at a Mach number of 2.0 was obtained at zero-lift conditions.